



HAL
open science

Non-ergodic fragmentation of protonated reserpine using femtosecond laser activation

Richard Brédy, Marius Hervé, Alexie Boyer, Jeffery Brown, Isabelle
Compagnon, Franck Lépine

► **To cite this version:**

Richard Brédy, Marius Hervé, Alexie Boyer, Jeffery Brown, Isabelle Compagnon, et al.. Non-ergodic fragmentation of protonated reserpine using femtosecond laser activation. *International Journal of Mass Spectrometry*, 2022, 471, pp.116729. 10.1016/j.ijms.2021.116729 . hal-03413791

HAL Id: hal-03413791

<https://hal.science/hal-03413791>

Submitted on 5 Jan 2024

HAL is a multi-disciplinary open access archive for the deposit and dissemination of scientific research documents, whether they are published or not. The documents may come from teaching and research institutions in France or abroad, or from public or private research centers.

L'archive ouverte pluridisciplinaire **HAL**, est destinée au dépôt et à la diffusion de documents scientifiques de niveau recherche, publiés ou non, émanant des établissements d'enseignement et de recherche français ou étrangers, des laboratoires publics ou privés.



Distributed under a Creative Commons Attribution - NonCommercial 4.0 International License

Non-ergodic fragmentation of protonated reserpine using femtosecond laser activation

Richard Brédy^{a,*}, *Marius Hervé*^{a,1}, *Alexie Boyer*^a, *Jeffery M Brown*^b, *Isabelle Compagnon*^a and
Franck Lépine^a

^a Univ Lyon, Université Claude Bernard Lyon 1, CNRS, Institut Lumière Matière, F-69622,
VILLEURBANNE, France

^b Waters Corporation, Stamford Avenue, Altrincham Road, Wilmslow, SK9 4AX, United Kingdom

***Corresponding Author**

richard.bredy@univ-lyon1.fr

Institut Lumière Matière (UMR 5306 CNRS)

10 rue Ada Byron

Campus Lyon Tech La Doua

Université Claude Bernard Lyon 1

69622 Villeurbanne cedex, France

Tel: +33 (0)4 72 44 83 68

¹ Present address: Univ. Rennes, CNRS, IPR (Institut de Physique de Rennes) – UMR 6251, F-35000 Rennes, France

Abstract

Specific fragmentation patterns are fingerprints that allow for unambiguous identification of molecules, for instance in analytical methods. To reveal and possibly control such specific fragmentation, it is essential to understand the physical processes involved during the activation step. We have performed “on-the-fly” (without trapping device) femtosecond (fs) laser activation / mass spectrometry experiments on gas phase protonated reserpine, a model molecular ion for analytical purpose, at different wavelengths and laser pulse intensities. In contrast to collision induced dissociation (CID) or 267 nm fs-laser activation, evidence of non-statistical fragmentation is observed when using 800 nm fs-laser activation. The associated mechanisms are discussed in terms of fragmentation induced by Coulomb repulsion after ultrafast ionization of the protonated molecule. Our results illustrate that the present “on-the-fly” experimental scheme can help in the understanding of the physics behind fs-laser activation.

Keywords: Fragmentation, mass spectrometry, reserpine, femtosecond

1. Introduction

Mass spectrometry techniques are widely used for analytical purpose of gas phase ions in the fields of proteomics [1], for peptide and protein characterization [2-4], DNA sequencing [5-7] and carbohydrates [8-12]. Based on molecular fragmentation, the analytical methods establish diagnostic fragmentation patterns to provide identification and structural characterization of biomolecules. Understanding the underlying excitation and fragmentation processes of these biomolecular ions is therefore of importance to manipulate, in a controlled manner, the fragmentation pathways and unambiguously identify biomolecular fingerprints. Based on this knowledge of molecular properties, new strategies or more sophisticated protocols may be elaborated to broaden the sequence coverage.

Various activation methods [2] have been developed to diversify the accessible fragmentation patterns. Among them, collision induced dissociation (CID) [13] is still one of the most common and easiest implemented methods, often used as a reference. CID relies on collisions with a gas of inert atoms that gradually convert part of the kinetic energy of the molecular ions of interest into internal energy leading, in general, to statistical fragmentation. As a result, the observed fragments originate from the cleavage of the weakest bonds after intramolecular energy redistribution. Similar mechanisms occur also, for instance, in infrared multiple photon dissociation (IRMPD) [14] techniques where the vibrational internal energy increase of the ion is due to multiple photon absorption. The weakest bonds prominence in statistical fragmentation appears then as a limitation in the sequence coverage. As many building blocks may not be observed, the potential gain on the structural information is reduced. Moreover, with molecules of increasing size, dissociation thresholds may not be reached as the internal energy is shared among a larger number of degrees of freedom. To overcome these limitations, complementary activation methods have been developed to target processes that involve non-statistical fragmentation pathways. These methods include for example various electron based techniques such as electron capture dissociation (ECD) or electron transfer dissociation (ETD) [15, 16], as well as excitation based on light interaction processes such as ultraviolet

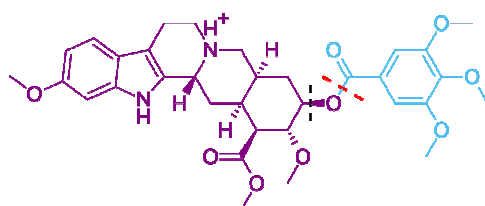
photodissociation (UVPD) [17], high energy photon/VUV/XUV irradiation [18, 19], or intense femtosecond laser interaction (fs-LID) [20].

With the advent of those activation methods, the question on the validity of the ergodic assumption for the observed fragmentation pathways has been raised. Non-ergodic processes frequently invoked to explain ECD/ETD of protonated peptide cations has been a matter of debates as various experimental results on peptide radical cations could be rationalized using statistical models or ab-initio theory without invoking non-ergodic assumption [16, 21, 22]. Both statistical and non statistical fragmentation have been reported in UV photodissociation [23-25] and the concept of nonergodic molecules was probed in femtosecond laser activation experiment [26, 27].

In the case of intense femtosecond laser interaction, a considerable amount of energy can be deposited in a molecule in a very short time. This especially leads to molecular ionization through the simultaneous absorption of more than one photons or tunnelling. The created radical may then fragment in a non-ergodic way, i.e., the timescale for the ultrafast bond cleavage does not allow for complete energy redistribution over the internal degrees of freedom of the ion. For instance, evidences for non-ergodic processes in mass-spectrometry experiments were observed using short laser pulse activation [20, 26-30]. The ultrashort activation time appears as a key parameter. It is suggested that the ultrafast creation of the radical cations plays a role and can induce selective reactions on a time scale faster than intramolecular energy redistribution.

Experiments involving photoactivation such as in fs-LID require an efficient coupling of the femtosecond laser with the molecular ions source and the mass spectrometer. Electrospray ionization (ESI) sources represent the technique of predilection for producing and transferring a large variety of molecular ions in the gas phase. In the current instruments, which are mostly designed for analytical purpose, ion trapping devices are usually required to compensate for the low ion density, to provide long activation time and to perform MSⁿ experiments. It is therefore not surprising that so far most photo-dissociation experiments have been conducted using ion trapping devices coupled to laser

systems with high repetition rate, in the kHz range. The long irradiation time, typically over tens of milliseconds, implies that the trapped molecular ions cloud experiences interaction with more than one laser pulse. Thus, unless special care is undertaken, ions and subsequent fragments may be activated by several laser pulses. By using relatively tight laser focus, the contribution of multiple interactions can be held on a relatively low level and determined statistically, thanks to the mixing of the trap content. However, multiple interaction processes cannot be completely ruled out and difficult to exclude at very high repetition rate. This raises questions when it comes to elucidate the primary fragmentation mechanisms using for example pump-probe schemes. Therefore, investigating the intrinsic processes at play during the very first steps of the fragmentation necessitates to ensure that each ion interacts, at most, with a single laser pulse. To achieve this condition, a cross beam configuration between a beam of molecular ions and a laser beam, without trapping device, may be used. With ion velocity in the order of few tens of m/s, typical interaction region of about 100 μm and laser repetition rate in the kHz range this “on-the-fly” type of experiment ensures that ions interact only once with the laser field, disentangling this interaction from “multiple-pulses” interactions. It is noteworthy that the strength of on-the-fly configuration also offers the possibility to implement techniques that are hard to access when using a trap, such as pump-probe experiments to study, for instance, fragmentation dynamics, measurements in coincidence or of quantities such as electron emission or kinetic energy release. Nonetheless, such on-the-fly spectroscopy is still challenging with molecular ions as it involves the production of a selected m/z parent ions beam with sufficient density coupled to a sensitive detection system over a wide dynamical range even at the signal-to-noise limit.



Scheme 1. Protonated reserpine [Res.H]⁺ (C₃₃H₄₀N₂O₉.H, m/z 609). The dash red bar indicates the O-R bond cleavage in the ester bridge leading to the specific fragments involved in non-ergodic fragmentation process: m/z 414 (coloured in purple) and m/z 195 (trimethoxybenzoyl group, coloured in blue). The dash black bar indicates the cleavage after the carboxyl moiety leading to fragment m/z 397 (see text).

We have performed on-the-fly fs-laser interaction experiment by coupling a femtosecond laser with a triple quadrupole instrument, i.e., without trapping device, to explore fragmentation processes on protonated reserpine (scheme 1). Reserpine is a model molecule, extensively used as a chemical standard to calibrate and evaluate performances of mass spectrometers. Extracted from the root of *Rauwolfia* species, reserpine is a monoterpene indole alkaloid that has been used as drug treatment for hypertension with potential side effects such as depression [31, 32]. With a pentacyclic core structure, the total synthesis of reserpine remains challenging [33]. Yet, reserpine has been used in mass spectrometry mostly from an analytical point of view to assess the fragmentation patterns for fingerprints identification or diagnostics [34-38]. Surprisingly very little is known about the physical properties of this molecule related to, for example, its electronic structure or its relaxation pathways dynamics.

In this work we propose to focus on the first steps of the interaction of a molecule with a single femtosecond laser pulse. We show that on-the-fly fs-laser interaction between protonated reserpine and 800 nm intense laser pulses leads to fragmentation processes triggered either by multiphoton ionization (MPI) or tunnel ionization (TI) depending on the considered laser intensities. The resulting fragmentation pathways are significantly different from the statistical ones observed in CID or by single photon resonant electronic excitation at 266 nm. Identification of some specific fragments sheds new light on the non-ergodic fragmentation occurring following fs-laser activation.

2. Material and methods

The experimental setup was based on a Xevo TQ-S micro triple-quadrupole instrument (Waters), modified to enable laser injection after the first quadrupole (Q1) [39] (SI Fig. S1). Reserpine ($C_{33}H_{40}N_2O_9$, $m = 608$ a.m.u.) purchased from Sigma-Aldrich was dissolved in MeOH:H₂O 1:1, with 0.1 % of acetic acid, at a concentration of 60 μ M. The solution was injected into vacuum by ESI, generating molecular ions in the gas phase. The ions of interests, here protonated reserpine, were selected according to their mass-to-charge ratio at m/z 609 using Q1 (MS1) and mass spectra were measured by scanning the last quadruple (Q2, MS2). Collision induced experiments were performed with argon gas in the T-wave collision cell (CC) at $P = 4 \times 10^{-3}$ mbar, and collision energy voltage from 0 to 30 V. For fs-laser experiments, ion activation was performed using a femtosecond laser delivering 800 nm ($h\nu = 1.55$ eV), 25 fs pulses, with an energy of 2 mJ at 5 kHz. The laser beam was injected orthogonally to the molecular ion beam and focused at the exit of the first quadrupole using a $f = 1$ m focal lens resulting in a calculated beam diameter of 130 μ m in the interaction region. At 800 nm mass spectra were recorded for laser intensities between 0 and 3.8×10^{14} W/cm² (maximum energy per pulse = 640 μ J). Additionally, pulses at 400 nm ($h\nu = 3.1$ eV) and 267 nm ($h\nu = 4.65$ eV) were produced by second- and third-harmonic generation (SHG and THG) from the 800 nm primary beam. Due to low conversion efficiency of the non-linear crystals used for SHG (about 15 %) and THG (about 2 %) mass spectra were recorded, after appropriate filtering, for a single energy per pulse at 400 nm (30 μ J/pulse, 1.5×10^{13} W/cm², 60 fs pulse duration) and at 267 nm (5 μ J/pulse, 2.8×10^{12} W/cm², 80 fs pulse duration). The calculated beam diameter in the interaction region at 400 nm and 267 nm was 90 μ m and 75 μ m, respectively. Typical ion velocity was on the order of 100 m/s in the interaction region delimited by the laser beam diameter at the focal point. Therefore, the ions were traveling several millimetres between two laser pulses separated in time by 200 μ s. This insures that an ion was interacting only once with the laser field. The overall background pressure inside the instrument was about 10^{-5} mbar, except inside the collision cell, where an argon pressure of 4×10^{-3} mbar is necessary to guide the ions with a

good transmission efficiency toward MS2, and to perform CID. For fs-laser experiments, the collision energy voltage was kept to 0 V to avoid interplay between CID and fs-laser interaction signals.

3. Results and discussion

Typical CID mass spectra with collision energy voltage set to 25 V and to 0 V are presented in Fig. 1. They are compared to mass spectra obtained using fs-laser interaction at 267 nm (5 $\mu\text{J}/\text{pulse}$, $2.8 \times 10^{12} \text{ W}/\text{cm}^2$), 400 nm (30 $\mu\text{J}/\text{pulse}$, $1.5 \times 10^{13} \text{ W}/\text{cm}^2$) and 800 nm (640 $\mu\text{J}/\text{pulse}$, $3.8 \times 10^{14} \text{ W}/\text{cm}^2$) (see also SI Fig. S3 to S6). Each spectrum is normalized to the total intensity. Fragmentation yields ($I_{\text{fragment}}/I_{\text{total}}$) for major or specific fragments are presented in supplementary material (SI Table ST1).

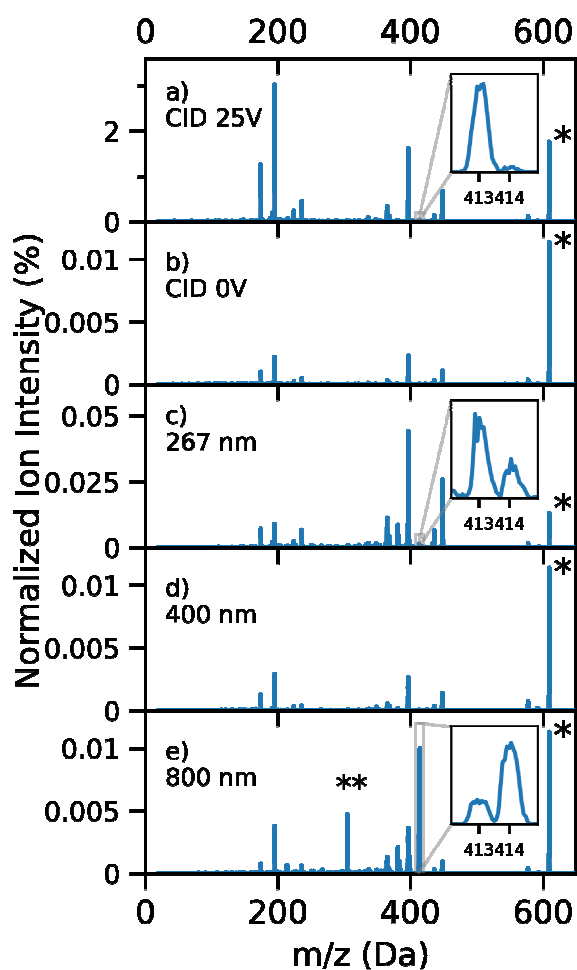


Fig. 1. Comparison of CID and fs-laser mass spectra of protonated reserpine (m/z 609). CID with collision energy voltage set to a) 25 V and b) 0 V, fs-laser interaction at c) 267 nm ($5 \mu\text{J}/\text{pulse}$, $2.8 \times 10^{12} \text{ W}/\text{cm}^2$), d) 400 nm ($30 \mu\text{J}/\text{pulse}$, $1.5 \times 10^{13} \text{ W}/\text{cm}^2$) and e) 800 nm ($640 \mu\text{J}/\text{pulse}$, $3.8 \times 10^{14} \text{ W}/\text{cm}^2$). Insets show the fragments at m/z 413 - 414. At 800 nm intact doubly charged reserpine ($[\text{Res.H}]^{*2+}$, m/z 304.5) is observed and marked by a double star (**). Peak of protonated reserpine parent ion at m/z 609 is marked by a star (*) and divided by a factor 1000 in b), c), d), e).

Fragments observed in CID mass spectra as a function of collision energy (SI Fig. S7 to S9) correspond to those observed in the literature [37, 38]. Below 30 V collision energy voltage, the dominant fragments are observed at m/z 174, 195, 397 and 448 (Fig. 1a). In particular, the fragment at m/z 397

corresponds to the bond cleavage after the carboxyl moiety (dash black bar in scheme 1), following nuclear rearrangements to give closed-shell products. The fragment at m/z 195, which corresponds to the trimethoxybenzoyl group (TMB), results from the fragmentation after the carbonyl moiety of the ester bridge (dash red bar in scheme 1). MS^n spectra of protonated reserpine in trap have shown that fragments at m/z 174 and 448 are generated due to C-ring cleavage via retro Diels Alder mechanism [37]. Breakdown curves extracted from CID mass spectra are presented in Fig. 2, showing the branching ratio dependence of the different fragmentation pathways with the collision energy. As collision energy voltage increases, smaller fragments appear due to higher excitation energy distribution and possible re-excitation of precursor ions as shown by the bell shape of the breakdown curves.

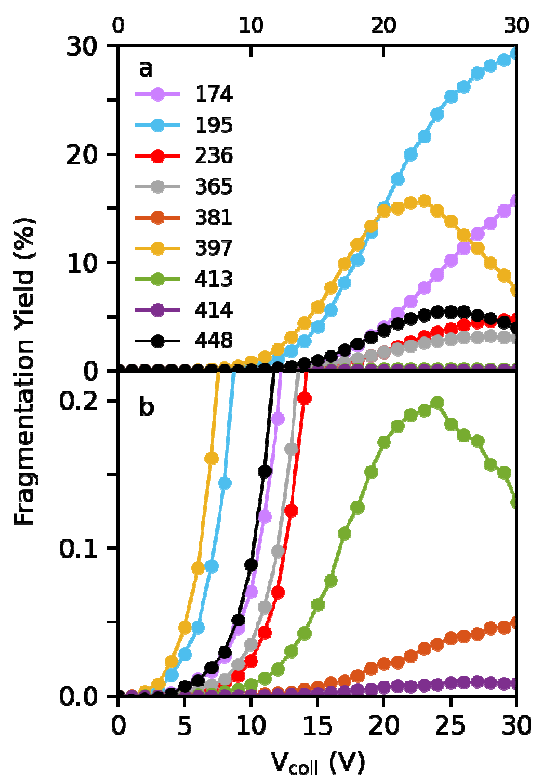


Fig. 2. CID breakdown curves as a function of collision energy voltage: a) for the major fragments at m/z 174 (light purple), 195 (TMB: light blue), 236 (red), 365 (grey), m/z 381 (orange), 397 (yellow), 413 (green), 414 (purple), and 448 (black); b) zoom showing the fragments of interest m/z 381 (orange), 413 (green) and 414 (purple).

Comparison of fs-laser interaction mass spectra at 267 nm, 400 nm and 800 nm show drastic changes in the fragmentation pattern as a function of the laser wavelength (Fig. 1c-e). It should be recalled that due to conversion efficiency in the generation of the 400 nm and 267 nm radiations from the 800 nm primary beam, intensity cannot be kept constant while varying the wavelength. This results in intensity variation of up to two orders of magnitude between 267 nm and 800 nm. Electronic absorption spectra of reserpine in solution exhibit strong absorption between 260 and 380 nm, depending on the solvent [40-42]. Precisely, two absorption bands have been identified, one at $\lambda_{\text{max}} \approx 295$ nm (S_1 state) and one at $\lambda_{\text{max}} \approx 270$ nm (S_2 state) in methanol as well as in 5 N acetic acid [40, 41], while in aqueous solution the absorption peaks at $\lambda_{\text{max}} \approx 292$ and 326 nm [42]. Though absorption bands can shift significantly for liquid or gas phase molecules, it is nonetheless expected that single photon absorption probability of gas phase protonated reserpine is higher at 267 nm than at 400 nm, and negligible at 800 nm. The fs-laser interaction mass spectrum at 267 nm presents clear fragmentation pattern with main fragments observed at m/z 397 and 448 (Fig. 1c). Overall, the fragmentation channels at 267 nm are similar to those observed in CID mass spectra, although the branching ratios are different. This suggests that fragmentation at this wavelength is mostly induced by statistical processes, due to resonant electronic excitation followed by internal conversion. Oppositely, absorption probability around 400 nm is weak (Fig. 1d) and no significant fragmentation induced by fs-laser interaction could be observed at this wavelength and peak laser intensity (1.5×10^{13} W/cm²). The negligible fragment signal observed in the corresponding mass spectrum is attributed mostly to residual fragmentation induced by collision with the background gas as suggested by mass spectra recorded without laser injection and collision energy voltage set to 0 V (Fig. 1b). This supports the absence of a resonant state at 400 nm. Mass spectra at 800 nm unambiguously reveals ion signal induced by laser interaction (Fig. 1e). Due to much higher laser peak intensity (3.8×10^{14} W/cm²), this signal is attributed to processes involving a large number of photons. It is therefore noteworthy that while some fragments, as m/z 195, are observed as in CID or 267 nm excitation, the 800 nm fs-laser interaction mass spectra present a different pattern with very specific fragments (SI Fig. S3). First of all, the radical dication (m/z 304.5) obtained by

photoionization of $[\text{Res.H}]^+$ is observed. This indicates that ionization of protonated reserpine can occur, leaving the molecule intact on the observation time window (on the order of few tens of milliseconds). It is noticeable that peak at m/z 304.5 is not observed in CID mass spectra nor at 267 nm. Secondly, the main fragment at m/z 414 observed in the 800 nm mass spectrum is observed with much lower probability in CID, which instead exhibits fragment at m/z 413 (see insets in Fig. 1 and SI Fig. S3). The fragment at m/z 414 corresponds exactly to the complement moiety of the TMB fragment (m/z 195), following cleavage of the O-R bond in the ester bridge (red bar in Scheme 1). As the complementary fragments at m/z 195 and 414 share the same bond cleavage, this strongly suggests that ionization of protonated reserpine can be followed by specific fragmentation of the radical dication $[\text{Res.H}]^{\bullet 2+}$ (Fig. 3a). It is suggested that m/z 414 fragment results from Coulomb repulsion of excited reserpine dication formed by ionization. Following the ultrafast ionization of protonated reserpine, the created radical dication might either remain stable with a lifetime on the order of few tens of milliseconds or fragment via both statistical and non-statistical processes depending on the internal energy. The reserpine dication carries two positive charges, one at the protonation site and one hole. In the case of fragmentation, the two charges may be shared between the two fragments at m/z 195 and 414 and fragmentation could occur without nuclear rearrangement, the largest moiety being for instance the protonated fragment (m/z 414) while the complement moiety (m/z 195) bears the hole. These processes are likely to occur in dication molecules due to the strong Coulomb repulsion, and may occur on ultrafast timescales.

The difference in fragmentation pathway of protonated reserpine leading to the different fragments at m/z 413 and 414 is proposed Fig. 3b. As fragment at m/z 414 corresponds to the O-R bond cleavage after the carbonyl group in the ester link, we suggest that dissociation leading to fragment at m/z 413 results from the same bond cleavage but with an additional hydrogen migration to the carbonyl moiety. This process would produce two fragments with closed-shell configurations, which is statistically more favourable and is more likely to occur in CID because of statistical vibrational energy redistribution. Oppositely, fragmentation pathway leading to the fragment at m/z 414 would not imply

closed-shell fragments and no nuclear rearrangement is necessary prior to dissociation. Therefore, using 800 nm intense short pulse fs-laser interaction on protonated reserpine can create radical species that result in different fragmentation patterns than statistically-activated protonated reserpine.

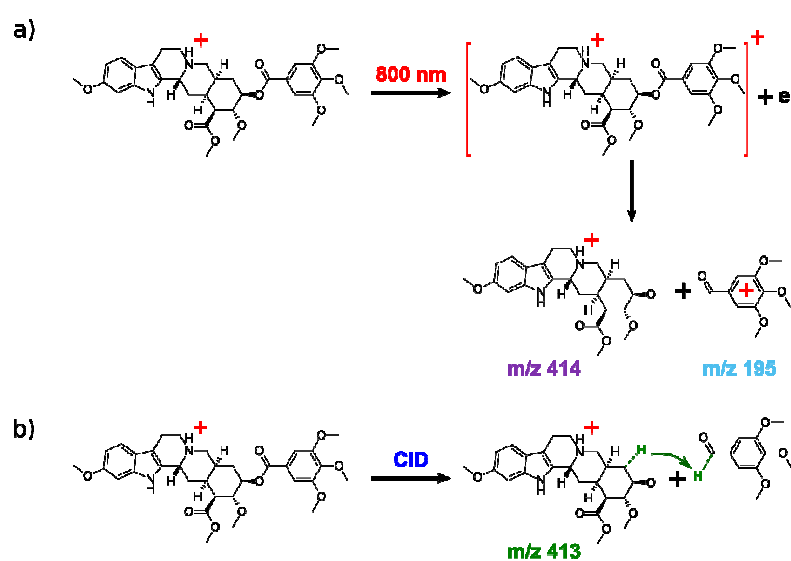


Fig. 3. Proposed fragmentation pathway of protonated reserpine $[\text{Res.H}]^+$: a) after 800 nm fs-laser interaction, protonated reserpine is ionized leading to reserpine dication $[\text{Res.H}]^{2+}$. Specific fragments at m/z 414 and 195 induced by Coulomb repulsion originate from the cleavage of the O-R bond in the ester bridge. b) in CID, fragment at m/z 413 results from the same O-R bond cleavage of the ester bridge followed by hydrogen migration to the carbonyl moiety, represented by the green arrow.

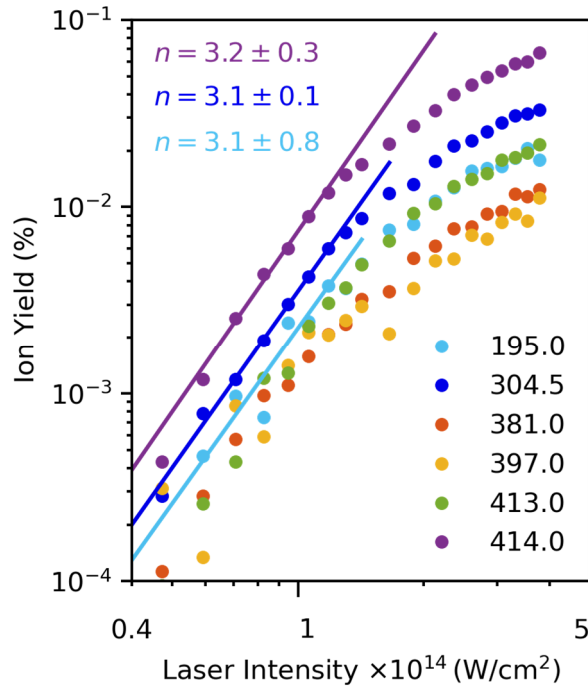


Fig. 4. Ion yield a function of peak intensity for 800 nm fs-laser pulse. Lines: power law fit $Y \propto I^n$ for reserpine dication (m/z 304.5, dark blue) and specific fragments at m/z 414 (purple) and 195 (light blue). The exponent n is related to the number of absorbed photons.

In intense fs-laser field, the ionization mechanism depends on the laser wavelength and intensity as well as on the ionization potential of the molecule. In strong field ionization processes of atomic gas information on the ionization regime is provided by the value γ of the Keldysh parameter [43-45]. Briefly, in the weak field regime (intensity $\ll 10^{14}$ W/cm 2 , $\gamma \gg 1$), multiphoton ionization as well as above-threshold ionization are the dominant processes. The ionization yield Y increases with the laser intensity and typically follows a power law $Y \propto I^n$, with the exponent n being related to the number of absorbed photons. In the strong field regime (intensity in the order or above 10^{14} W/cm 2 , $\gamma \ll 1$), the ionization is driven by tunneling effect and the ionization yield reaches a saturation value. In order to understand the underlying process involved in this current work, the evolution of the fragmentation yield has been recorded as a function of the laser pulse intensity for 800 nm excitation wavelength.

The result is presented in Fig. 4 for the main fragments, for laser intensities between $3.5 \times 10^{13} \text{ W/cm}^2$ and $3.8 \times 10^{14} \text{ W/cm}^2$. These intensities cover the range from resonant multiphoton ionization to tunnel ionization regime ($1.4 > \gamma > 0.4$, for IP = 8 eV). In the double-logarithmic representation of Fig. 4, a similar trend is observed for all the ion yields that increase with the increasing laser peak intensity. For intensities between $3.5 \times 10^{13} \text{ W/cm}^2$ and $1.2 \times 10^{14} \text{ W/cm}^2$, the increase of the ion yields follows a power law as shown for the dication (m/z 304.5, $n = 3.1 \pm 0.1$), fragments at m/z 195 ($n = 3.1 \pm 0.8$) and 414 ($n = 3.2 \pm 0.3$). Above $1.2 \times 10^{14} \text{ W/cm}^2$, the ion yields deviate from the power law toward a saturation value which indicates that focal volume and tunnelling effects start to become non-negligible [30, 43]. This laser intensity dependence suggests that a transition from MPI to TI processes is indeed observed in the intensity range considered in this work. It is noteworthy that in this laser intensity range, ionization of protonated reserpine occurs and could lead to non-ergodic fragmentation. This is in line with the idea that ultrafast ionization is one of the key parameters that could trigger specific fragmentation.

To our knowledge, the ionization potential of protonated reserpine has neither been measured nor calculated. It is expected to lie above the IP = 7.88 eV of the neutral reserpine [46] due to Coulombic effect of the added proton and/or structure modification, this was for instance observed in the case of polypeptides [47, 48]. In 800 nm multiphoton ionization, at least 5 photons would be required to reach this ionization potential ($5 \times hv = 7.75 \text{ eV} \sim 7.88 \text{ eV}$). However, the number of photons (3 to 4) extracted from the slope of the reserpine dication m/z 304.5 is lower. This is a characteristic signature of the existence of an intermediate electronic state lying below the IP, such excited electronic states being resonant with a multiple of the fundamental 800 nm photon energy. Consequently, the production of reserpine dication at 800 nm may be influenced by resonance-enhanced multiphoton ionization (REMPI). In that case, the number of photons deduced from the slope of the dication yield in Fig. 4 would reflect the probability to excite the intermediate state from the ground state (S_0) followed by a transition to the continuum. This is consistent with the absorption band at $\lambda_{\text{max}} \approx 270 \text{ nm}$, which may be resonant with three photons absorption at 800 nm. This suggests that the

intermediate state plays a role in both 267 nm and 800 nm excitation of protonated reserpine, involving one 267 nm photon ($h\nu = 4.65$ eV formed by third-harmonic generation) or three 800nm photons ($h\nu = 1.55$ eV). At 800 nm, due to higher intensity, this resonant intermediate electronic state would be populated by 3 photon absorption ($3 \times h\nu = 4.65$ eV), immediately followed by the absorption of at least two or three photons ($2 \times h\nu = 3.1$ eV) to reach the ionization potential of the protonated reserpine from the intermediate excited state ($4.65 + 3.1 = 7.75$ eV \sim IP) (see Fig. 5). Therefore, the power law exponents in the low intensity range strongly support the assumption of an intermediate excited electronic state involved in the ionization process.

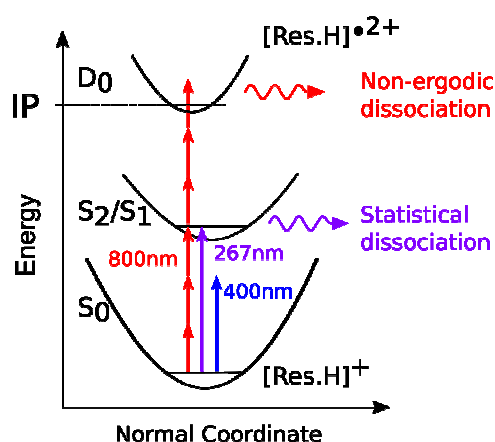


Fig. 5. Schematic interpretation of protonated reserpine $[\text{Res.H}]^+$ excitation at 800 nm (MPI) and 267 nm (single photon absorption). Interaction at 400 nm is off resonance leading to no fragmentation at the considered laser intensity.

The major fragment at m/z 414 appears to be specific to 800 nm fs-laser activation method, while it is almost negligible with CID method. However, the fragment at m/z 413, which differs by only one a.m.u., is observed with substantial intensity in both mass spectra. It is therefore noticeable that the yield ratio $R = Y_{414}/Y_{413} \sim 3.3$ is nearly independent of laser intensity in the 800 nm experiments while it is inverted and changes drastically with collision energy in CID (see green and purple curves in Fig. 2 and 4). From the ion yield evolution of fragments at m/z 195 and 414 in Fig. 4, the same apparent number of photons ($n \approx 3$) is required to induce fragmentation as to ionize the protonated reserpine. This suggests that the fragmentation pathway of protonated reserpine that leads to fragment m/z 414 cannot be explained by statistical excitation of the molecule, as it would be the case in CID, and supports the proposed fragmentation scheme of Fig. 3. In laser interaction at 266 nm and in the MPI regime at 800 nm, due to the excitation of the intermediate resonant state, the probability to ionize or to dissociate protonated reserpine is determined by the probability to absorb extra photons from this excited state. While the intermediate state is involved in both 266 nm and 800 nm excitations, the intensity-driven single- versus multiphoton process leads to different fragmentation pathways. At 266 nm, no supplementary absorption from the excited state is observed and internal vibrational energy redistribution from the intermediate state induces statistical fragmentation. At 800 nm, ionization occurs because of additional photon absorption from the intermediate state, and is eventually followed by non-ergodic fragmentation. The implication of the intermediate state in the fragmentation of protonated reserpine may also explain the absence of fragmentation observed at 400 nm ($h\nu = 3.1$ eV) with laser intensity too low to reach the multiphoton regime.

Regarding fragmentation at 800 nm, it is noteworthy that the mass spectrum does not show strong variations within the intensity range of this study. The low ion yield values in Fig. 4 and their evolution as a function of laser intensity support the interpretation that fragments are generated mostly from the dication and not from the monocation.

4. Conclusions

Mass spectra of protonated reserpine were obtained using on-the-fly fs-laser/MS experiment at 267 nm, 400 nm and 800 nm and compared with CID activation method. In contrast to experiments based on ion trapping devices, the on-the-fly experimental configuration may favour elucidation of the primary molecular processes involved in the fragmentation mechanisms by allowing, for example, dynamics measurements in pump-probe experiments. Mass spectra at 800 nm fs-laser interaction exhibits very specific fragmentation patterns as well as ionization of the protonated reserpine over a wide range of laser intensities. Activation at 267 nm leads to fragments similar to CID while negligible fragmentation induced by 400 nm fs-laser interaction is observed at the considered laser intensity. The specific fragment m/z 414 observed at 800 nm fs-laser activation is interpreted as due to non-ergodic process triggered by the ultrafast ionization of the protonated reserpine. This ionization can be initiated either by multiphoton or tunnel ionization. Due to the ultrafast increase of the charge, the formed radical dication can fragment through different major channels that differ and may occur much more rapidly than those observed by statistical energy redistribution processes as in CID or 267 nm activation. Interpretation of the results involves the excitation of an intermediate resonant state of protonated reserpine for both 267 nm and 800 nm activation. At the considered laser intensity, single photon absorption at 267 nm preferentially leads to internal energy redistribution while at 800 nm the excited state acts as an intermediate state in the multiphoton ionization process. This single vs many photon aspect suggests that different fragmentation patterns may be laser-intensity-driven. These results could contribute to comprehend the mechanisms involved in analytical methods based on short intense laser interaction. The key point is related to the ultrafast ionization of the protonated molecule that unveils new fragmentation channels due to the Coulomb repulsion between the proton site and the extra-created charge. By understanding the underlying mechanisms involved in such activation methods, specific fragmentation channels may be controlled to help unravelling molecular fingerprints for analytical purpose. These results illustrate the use of ultrafast processes to control bond cleavages in the goal of unambiguously elucidate the molecular structures. Beside the analytical interest, the

observation of such specific fragmentation also offers the possibility to study the dynamics of the involved excited states. This kind of studies could unequivocally provide conclusion on the non-ergodic nature of the involved processes and may be of help towards a better understanding of reserpine interactions such as oxidation [35] or in drug receptor mechanism via charge transfer [40].

Acknowledgments: This work was supported by CNRS and ANR-16-CE30-0012 "Circé".

References

- [1] R. Aebersold, D. R. Goodlett, Mass spectrometry in proteomics, *Chem. Rev.* 101 (2001) 269–296. <https://doi.org/10.1021/cr990076h>.
- [2] J. S. Brodbelt, Ion activation methods for peptides and proteins, *Anal. Chem.* 88 (2016) 30–51. <https://doi.org/10.1021/acs.analchem.5b04563>.
- [3] A. P. Jonsson, Mass spectrometry for protein and peptide characterisation, *Cell. Mol. Life Sci.* 58 (2001) 868–884. <https://doi.org/10.1007/PL00000907>.
- [4] V. H. Wysocki, K. A. Resing, Q. Zhang, G. Cheng, Mass spectrometry of peptides and proteins, *Methods* 35 (2005) 211–222. <https://doi.org/10.1016/j.ymeth.2004.08.013>.
- [5] J. R. Edwards, H. Ruparel, J. Ju, Mass-spectrometry DNA sequencing, *Mutat. Res-Fund. Mol. M.* 573 (2005) 3–12. <https://doi.org/10.1016/j.mrfmmm.2004.07.021>.
- [6] H. Köster, K. Tang, D.-J. Fu, A. Braun, D. v. d. Boom, C. L. Smith, R. J. Cotter, C. R. Cantor, A strategy for rapid and efficient DNA sequencing by mass spectrometry, *Nat. Biotechnol.* 14 (1996) 1123–1128. <https://doi.org/10.1038/nbt0996-1123>.
- [7] J. Tost, I. G. Gut, DNA analysis by mass spectrometry-past, present and future, *J. Mass Spectrom.* 41 (2006) 981–995. <https://doi.org/10.1002/jms.1096>.
- [8] J. Zaia, Mass spectrometry of oligosaccharides, *Mass Spectrom. Rev.* 23 (2004) 161–227. <https://doi.org/10.1002/mas.10073>.
- [9] L. Han, C. E. Costello, Mass spectrometry of glycans, *Biochemistry (Mosc)* 78 (2013) 710–720. <https://doi.org/10.1134/S0006297913070031>.

- [10] M. J. Kailemia, L. R. Ruhaak, C. B. Lebrilla, I. J. Amster, Oligosaccharide analysis by mass spectrometry: A review of recent developments, *Anal. Chem.* 86 (2014) 196–212.
<https://doi.org/10.1021/ac403969n>.
- [11] E. Mirgorodskaya, N. G. Karlsson, C. Sihlbom, G. Larson, C. L. Nilsson, Cracking the sugar code by mass spectrometry, *J. Am. Soc. Mass Spectrom.* 29 (2018) 1065–1074.
<https://doi.org/10.1007/s13361-018-1912-3>.
- [12] B. Schindler, L. Barnes, G. Renois, C. Gray, S. Chambert, S. Fort, S. Flitsch, C. Loison, A.-R. Allouche, I. Compagnon, Anomeric memory of the glycosidic bond upon fragmentation and its consequences for carbohydrate sequencing, *Nat Commun* 8 (2017) 973.
<https://doi.org/10.1038/s41467-017-01179-y>.
- [13] J. Mitchell Wells, S. A. McLuckey, Collision-induced dissociation (CID) of peptides and proteins, *Meth. Enzymol.* 402 (2005) 148–185. [https://doi.org/10.1016/S0076-6879\(05\)02005-7](https://doi.org/10.1016/S0076-6879(05)02005-7).
- [14] N. C. Polfer, Infrared multiple photon dissociation spectroscopy of trapped ions, *Chem. Soc. Rev.* 40 (2011) 2211–2221. <https://doi.org/10.1039/C0CS00171F>.
- [15] K. Breuker, H. Oh, C. Lin, B. K. Carpenter, F. W. McLafferty, Nonergodic and conformational control of the electron capture dissociation of protein cations, *Proc. Natl. Acad. Sci.* 101 (2004) 14011–14016. <https://doi.org/10.1073/pnas.040609510>.
- [16] F. Lermyte, D. Valkenburg, J. A. Loo, F. Sobott, Radical solutions: Principles and application of electron-based dissociation in mass spectrometry-based analysis of protein structure, *Mass Spectrom. Rev.* 37 (2018) 750–771. <https://doi.org/10.1002/mas.21560>.
- [17] J. S. Brodbelt, Photodissociation mass spectrometry: new tools for characterization of biological molecules, *Chem. Soc. Rev.* 43 (2014) 2757–2783. <https://doi.org/10.1039/C3CS60444F>.

- [18] S. Bari, O. Gonzalez-Magaña, G. Reitsma, J. Werner, S. Schippers, R. Hoekstra, T. Schlathöler, Photodissociation of protonated leucine-enkephalin in the VUV range of 8-40 eV, *J. Chem. Phys.* 134 (2011) 024314. <https://doi.org/10.1063/1.3515301>.
- [19] A. Giuliani, J. P. Williams, M. R. Green, Extreme ultraviolet radiation: A means of ion activation for tandem mass spectrometry, *Anal. Chem.* 90 (2018) 7176–7180. <https://doi.org/10.1021/acs.analchem.8b01789>.
- [20] C. L. Kalcic, T. C. Gunaratne, A. D. Jones, M. Dantus, G. E. Reid, Femtosecond laser-induced ionization/dissociation of protonated peptides, *J. Am. Chem. Soc.* 131 (2009) 940–942. <https://doi.org/10.1021/ja8089119>.
- [21] F. Turecek, R. R. Julian, Peptide radicals and cation radicals in the gas phase, *Chem. Rev.* 113 (2013) 6691–6733. <https://doi.org/10.1021/cr400043s>.
- [22] J. Laskin, J. H. Futrell, I. K. Chu, Is dissociation of peptide radical cations an ergodic process?, *J. Am. Chem. Soc.* 129 (2007) 9598–9599. <https://doi.org/10.1021/ja073748r>.
- [23] G. Grégoire, H. Kang, C. Dedonder-Lardeux, C. Jouvet, C. Desfrancois, D. Onidas, V. Lepere, J. A. Fayeton, Statistical vs. non-statistical deactivation pathways in the UV photo-fragmentation of protonated tryptophan-leucinedipeptide, *Phys. Chem. Chem. Phys.* 8 (2006) 122–128. <https://doi.org/10.1039/b510406h>.
- [24] C. S. Byskov, F. Jensen, T. J. D. Jørgensen, S. B. Nielsen, On the photostability of peptides after selective photoexcitation of the backbone: prompt versus slow dissociation, *Phys. Chem. Chem. Phys.* 16 (2014) 15831–15838. <https://doi.org/10.1039/c4cp02015d>.
- [25] R. R. Julian, The mechanism behind top-down UVPD experiments: Making sense of apparent contradictions, *J. Am. Soc. Mass Spectrom.* 28 (2017) 1823–1826. <https://doi.org/10.1007/s13361-017-1721-0>.

- [26] E. W. Diau, J. L. Herek, Z. H. Kim, A. H. Zewail, Femtosecond activation of reactions and the concept of nonergodic molecules, *Science* 279 (1998) 847–851.
<https://doi.org/10.1126/science.279.5352.847>.
- [27] T. I. Sølling, T. S. Kuhlman, A. B. Stephansen, L. B. Klein, K. B. Møller, The non-ergodic nature of internal conversion, *ChemPhysChem* 15 (2013) 249–259.
<https://doi.org/10.1002/cphc.201300926>.
- [28] C. L. Kalcic, G. E. Reid, V. V. Lozovoy, M. Dantus, Mechanism elucidation for nonstochastic femtosecond laser-induced ionization/dissociation: From amino acids to peptides, *J. Phys. Chem. A* 116 (2012) 2764–2774. <https://doi.org/10.1021/jp208421d>.
- [29] C. Neidel, A. Kuehn, C. P. Schulz, I. V. Hertel, M. W. Linscheid, T. Schultz, Femtosecond laser-induced dissociation (fs-LID) as an activation method in mass spectrometry, *Chem. Phys.* 514 (2018) 106–112. <https://doi.org/10.1016/j.chemphys.2018.05.008>.
- [30] G. Reitsma, O. Gonzalez-Magaña, O. Versolato, M. Door, R. Hoekstra, E. Surraud, B. Fischer, N. Camus, M. Kremer, R. Moshhammer, T. Schlathölter, Femtosecond laser induced ionization and dissociation of gas-phase protonated leucine enkephalin, *Int. J. Mass spectrom.* 365-366 (2014) 365–371. <https://doi.org/10.1016/j.ijms.2014.01.004>.
- [31] T. Hedgecock, A. Phillips, B. Ludrick, T. Golden, N. Wu, Molecular mechanisms and applications of a reserpine-induced rodent model, *SSR Inst. Int. J. Life Sci.* 5 (2019) 2160–2167.
<https://doi.org/10.21276/ssr-ijls.2019.5.1.8>.
- [32] S. D. Shamon, M. I. Perez, Blood pressure-lowering efficacy of reserpine for primary hypertension, *Cochrane Db. Syst. Rev.* 12 (2016) CD007655.
<https://doi.org/10.1002/14651858.cd007655.pub3>.
- [33] F.-E. Chen, J. Huang, Reserpine: A challenge for total synthesis of natural products, *Chem. Rev.* 105 (2005) 4671–4706. <https://doi.org/10.1021/cr050521a>.

- [34] M. A. Anderson, T. Wachs, J. D. Henion, Quantitative ionspray liquid chromatographic/tandem mass spectrometric determination of reserpine in equine plasma, *J. Mass Spectrom.* 32 (1997) 152–158. [https://doi.org/10.1002/\(sici\)1096-9888\(199702\)32:2<152::aid-jms456>3.0.co;2-w](https://doi.org/10.1002/(sici)1096-9888(199702)32:2<152::aid-jms456>3.0.co;2-w).
- [35] J. A. Fournier, A. B. Wolk, M. A. Johnson, Integration of cryogenic ion vibrational predissociation spectroscopy with a mass spectrometric interface to an electrochemical cell, *Anal. Chem.* 85 (2013) 7339–7344. <https://doi.org/10.1021/ac401228y>.
- [36] M. Iqbal, A. Alam, T. A. Wani, N. Y. Khalil, Simultaneous determination of reserpine, rescinnamine, and yohimbine in human plasma by ultraperformance liquid chromatography tandem mass spectrometry, *J. Anal. Methods Chem.* 2013 (2013) 1–11. <https://doi.org/10.1155/2013/940861>.
- [37] S. Kumar, A. Singh, V. Bajpai, B. Kumar, Identification, characterization and distribution of monoterpene indole alkaloids in *Rauwolfia* species by Orbitrap Velos Pro mass spectrometer, *J. Pharm. Biomed. Anal.* 118 (2016) 183–194. <https://doi.org/10.1016/j.jpba.2015.10.037>.
- [38] S. Kumar, A. Singh, V. Bajpai, M. Srivastava, B. P. Singh, B. Kumar, Structural characterization of monoterpene indole alkaloids in ethanolic extracts of *Rauwolfia* species by liquid chromatography with quadrupole time-of-flight mass spectrometry, *J. Pharm. Anal.* 6 (2016) 363–373. <https://doi.org/10.1016/j.jpha.2016.04.008>.
- [39] M. Hervé, R. Brédy, G. Karras, B. Concina, J. Brown, A.-R. Allouche, F. Lépine, I. Compagnon, On-the-fly femtosecond action spectroscopy of charged cyanine dyes: Electronic structure versus geometry, *J. Phys. Chem. Lett.* 10 (2019) 2300–2305. <https://doi.org/10.1021/acs.jpcclett.9b00435>.
- [40] H. H. Eldaroti, S. A. Gadir, M. S. Refat, A. M. A. Adam, Spectroscopic investigations of the charge-transfer interaction between the drug reserpine and different acceptors: Towards

understanding of drug–receptor mechanism, *Spectrochim. Acta Part A Mol. Biomol. Spectrosc.* 115 (2013) 309–323. <https://doi.org/10.1016/j.saa.2013.06.046>.

[41] E. H. Sakal, E. J. Merrill, Ultraviolet spectrophotometric determination of reserpine, *J. Am. Pharm. Assoc.* 43 (1954) 709–715. <https://doi.org/10.1002/jps.3030431203>.

[42] B. C. Ghosh, N. Deb, A. K. Mukherjee, Determination of individual proton affinities of reserpine from its UV-vis and charge-transfer spectra, *J. Phys. Chem. A* 112 (2008) 6929–6935. <https://doi.org/10.1021/jp802082y>.

[43] J. H. Posthumus, The dynamics of small molecules in intense laser fields, *Rep. Progr. Phys.* 67 (2004) 623–665. <https://doi.org/10.1088/0034-4885/67/5/r01>.

[44] L. V. Keldysh, Ionization in the field of a strong electromagnetic wave, *Sov. Phys. JETP* 20 (1965) 1307.

[45] K. Amini, J. Biegert, F. Calegari, A. Chacón, M. F. Ciappina, A. Dauphin, D. K. Efimov, C. F. de Morisson Faria, K. Giergiel, P. Gniewek, A. S. Landsman, M. Lesiuk, M. Mandrysz, A. S. Maxwell, R. Moszynski, L. Ortmann, J. A. Pérez-Hernández, A. Picón, E. Pisanty, J. Prauzner-Bechcicki, K. Sacha, N. Suárez, A. Zaïr, J. Zakrzewski, M. Lewenstein, Symphony on strong field approximation, *Rep. Progr. Phys.* 82 (2019) 116001. <https://doi.org/10.1088/1361-6633/ab2bb1>.

[46] M. A. Slifkin, A. C. Allison, Measurement of ionization potentials from contact charge transfer spectra, *Nature* 215 (1967) 949–950. <https://doi.org/10.1038/215949a0>.

[47] B. A. Budnik, Y. O. Tsybin, P. Håkansson, R. A. Zubarev, Ionization energies of multiply protonated polypeptides obtained by tandem ionization in Fourier transform mass spectrometers, *J. Mass Spectrom.* 37 (2002) 1141–1144. <https://doi.org/10.1002/jms.376>.

[48] A. Giuliani, A. R. Milosavljevic, K. Hinsen, F. Canon, C. Nicolas, M. Réfrégiers, L. Nahon, Structure and charge-state dependence of the gas-phase ionization energy of proteins, *Angew. Chem. - Int. Ed.* 51 (2012) 9552–9556. <https://doi.org/10.1002/anie.201204435>.